Thin Solid Films 517 (2008) 943–947

Contents lists available at ScienceDirect

Thin Solid Films

journal homepage: www.elsevier.com/locate/tsf

A morphologically stable host material for efficient phosphorescent green and red organic light emitting devices

Meng-Huan Ho [a,*], Banumathy Balaganesan [a], Ta-Ya Chu [b], Teng-Ming Chen [a], Chin H. Chen [c]

[a] Department of Applied Chemistry, National Chiao Tung University, Hsinchu, 300, Taiwan, ROC
[b] Department of Electrophysics, National Chiao Tung University, Hsinchu, 300, Taiwan, ROC
[c] Display Institute, Microelectronics and Information Systems Research Center, National Chiao Tung University, Hsinchu, 300, Taiwan, ROC

ARTICLE INFO

Article history:
Received 26 June 2007
Received in revised form 5 June 2008
Accepted 13 July 2008
Available online 19 July 2008

Keywords:
Organic electroluminescent devices
Phosphorescence
Host material
Carbazole

ABSTRACT

A carbazole-based host material, 4,4′-*N*,*N*′-[di(3, 6-di(*t*-butyl)carbazole]biphenyl (ttbCBP), with four *t*-butyl steric spacers on peripheral carbazole moieties was effectively synthesized through Friedel–Crafts Alkylation. Owing to the presence of sterically hindered *t*-butyl groups, ttbCBP exhibits a high glass transition temperature (175 °C) and is morphologically stable. This host material also preserves the characteristics of wide band-gap of 3.2 eV and high triplet energy of 2.64 eV. In addition, ttbCBP has been shown to be effective hosts for green and red phosphorescent emitters in organic electrophosphorescent devices.

1. Introduction

Recently, high-efficiency organic light emitting diodes (OLEDs) have been demonstrated due to the harvest of both singlet and triplet excitons of phosphorescent emitters [1–4]. The phosphorescence from the devices can be understood in terms of the energy transfer from both the singlet and triplet excited states of the host materials to the triplet excited states of the phosphorescent guest molecules and/or by direct excitation of the phosphorescent guest molecules by charge trapping. Both of these mechanisms are capable of producing nearly 100% internal quantum efficiency. However, it is essential for host materials to possess high triplet energy to prevent from back energy transfer and confine triplet exciton on guest molecules [5,6].

For OLEDs, a prominent class of materials that fulfills the above-mentioned boundary conditions is the class of carbazoles. A common carbazole derivative that is often used as host for triplet emitters is *N*, *N*′-dicarbazolyl-4,4′-biphenyl (CBP), resulting in maximum internal quantum efficiencies of 60 to 80% for green and red triplet emitters [3,7–11]. When doping with the green phosphor *fac*-tris(2-phenylpyridine)iridium ($Ir(ppy)_3$) [7] and red phosphor tris(2-(2′benzo[4,5-a]thienyl)pyridinato-*N*,$C^{3'}$) iridium (acethylacetonate) [8], high external quantum efficiency (E. Q. E.) of 7.5% and 7.0% can be achieved, respectively.

Although the triplet energy is an important factor for host materials applied in phosphorescent OLEDs, the morphological stability of host materials should also be considered [12,13]. To have a large energy gap, the extent of conjugation in the molecule must be limited, which in turn would usually impose considerable constraints in molecular size and weight. However, the reduced molecular size restricts the thermal stability of molecules and further makes molecules difficult to form morphologically stable and uniform thin films. Several studies have indicated that the thermal and morphological instabilities of host materials may shorten the operational lifetime of devices [14]. Therefore, various studies have been focused on hybridizing carbazole moiety with some bulky and steric groups, like triphenylsilane [15], fluorene [16], or *tert*-butyl benzene [17,18], to improve the thermal and morphological stability of the carbazole-based host materials and applied in electrophosphorescent OLEDs.

Recently, Chen et al. reported the synthesis of a 3,6-di(*t*-butyl) CBP with high triplet energy via several synthetic steps [19]. In this paper, we describe a simple, convenient and efficient synthesis of a *tetra*(*t*-butyl)-substituted carbazole derivative directly from CBP, 4,4′-*N*,*N*′-[di(3, 6-di(*t*-butyl)carbazole]biphenyl, (abbreviated as ttbCBP), bearing the *t*-butyl groups at C-3, C-6, C-3′, and C-6′ carbon atoms on both carbazole moieties of CBP. This synthetic procedure furnished high yields of ttbCBP with high purity. We propose the sterically hindered *t*-butyl spacers can avoid the formation of polycrystalline films and improve the thermal properties. This host material also preserves the characteristics of wide band-gap and high triplet energy, both of which are important in the confinement of triplet exciton on the guest molecules, thus is suitable as a host material for green and red electrophosphorescent devices.

* Corresponding author. Tel.: +886 3 5712121x52919; fax: +886 3 573 5601.
E-mail address: kinneas.ac94g@nctu.edu.tw (M.-H. Ho).

0040-6090/$ – see front matter © 2008 Elsevier B.V. All rights reserved.
doi:10.1016/j.tsf.2008.07.005

2. Experimental section

The *tetra*(*t*-butyl)-substituted compound, ttbCBP, was synthesized by Friedel–Crafts Alkylation [20] as depicted in Scheme 1. A mixture of CBP (1.0 equiv) and *tert*-butyl chloride (4.2 equiv) were dissolved in dichloromethane and heated to reflux at 80 °C while anhydrous $AlCl_3$ (20 mol%) was added slowly into the mixture and reflux was continued. The reaction was monitored by thin-layer chromatography [2% ethyl acetate (EA) in *n*-hexane]. After 30 min of reflux, the mixture was poured into ice-water and extracted with EA. The organic layer was washed with water several times and dried with anhydrous Na_2SO_4. After rotary evaporation, the crude product was washed with *n*-hexane to get >90% pure white–yellow solid (yield ~75%). The crude product was further purified via train sublimation and its purity was thoroughly checked by high-performance liquid chromatography to be >99%. The molecular structure of ttbCBP was characterized by ^1H and ^{13}C nuclear magnetic resonance, mass spectra, and elemental analyses.

ttbCBP. ^1H NMR (300 MHz, $CDCl_3$): δ/ppm 1.47 (s, 36H), 7.41–7.50 (m, 8H), 7.66–7.69 (d, 4H), 7.86–7.89 (d, 4H), 8.14–8.15 (d, 4H). FAB-MS: *m*/*z*=708 (M^+). Anal. for $C_{50}H_{40}N_2$: Calcd: C, 88.09; H, 7.96; N, 3.95. Found: C, 88.37; H, 7.61; N, 3.76.

Differential scanning calorimetry (DSC) was performed using a Seiko SSC 5200 instrument operated at heating and cooling rates of 10 and 30 °C/min, respectively. Samples were scanned from 30 to 400 °C, cooled to 30 °C, and then scanned again from 30 to 400 °C; the glass transition temperatures (T_g) were determined from the second heating scan. Thermogravimetric analysis (TGA) was undertaken on a Seiko TG/DTA 200 instrument under a nitrogen atmosphere, by measuring weight loss while heating at a rate of 10 °C/min. UV–Vis and photoluminescence spectra were measured by Hewlett Packard 8453 and Acton Research Spectra Pro-150, respectively. The ionization potential was determined by the UV photoelectron spectroscopy (Model AC-2). The calculated electron distribution of highest occupied molecular orbital/lowest occupied molecular orbital (HOMO/LUMO) levels were optimized by *ab initio* density functional theory (DFT) with the B3LYP/6-31G* basis sets [21] in Gaussian 03 program [22].

To demonstrate the efficacy of ttbCBP, the following devices have been fabricated. Green devices: Indium tin oxide (ITO)/CF_x/*N*,*N*′-bis(1-naphthyl)-*N*,*N*′-diphenyl-1,1′-biphenyl-4,4′-diamine (NPB) (60 nm)/ 7% $Ir(ppy)_3$ doped in ttbCBP (Device *A*) or CBP (Device *B*) (30 nm)/ 4,7-diphenyl-1,10-phenanthroline (BPhen) (30 nm)/tris(8-quinolinolato) aluminium (Alq_3) (15 nm)/LiF (1 nm)/Al (200 nm); Red devices: ITO/ CF_x/NPB (60 nm)/9% tris(1-phenylisoquinolinato-C^2,N)iridium(III) (Ir(piq)$_3$) [11] doped in ttbCBP (Device *C*) or CBP (Device *D*) (50 nm)/ BPhen (10 nm)/Alq_3 (35 nm)/LiF (1 nm)/Al (200 nm). CF_x, NPB, Alq_3 and LiF were used as the hole injection material [23], hole and electron transport materials and electron injection material, respectively. A thin layer of BPhen was inserted between the EML and electron-transporting layer as the hole-blocking and exciton-blocking layer to provide the carrier and exciton confinement.

After a routine cleaning procedure, the ITO-coated glass was loaded on the grounded electrode of a parallel-plate plasma reactor, pretreated by oxygen plasma, and then coated with a polymerized fluorocarbon film. Devices were fabricated under the base vacuum of about 5×10^{-4} Pa in a thin-film evaporation coater following a published protocol [24]. In the evaporation of EML, the phosphorescent dopant was co-deposited at its optimal molar ratio. All devices were hermetically sealed prior to testing. The active area of the EL device, defined by the overlap of the ITO and the cathode electrodes, was 9 mm^2. The current–voltage–luminance characteristics of the devices were measured with a diode array rapid scan system using a Photo Research PR650 spectrophotometer and a computer-controlled programmable direct current source.

Table 1
Thermal and photophysical properties of CBP and ttbCBP

Material	T_g (°C)	T_m (°C)	T_d (°C)	$\lambda_{abs,\ max}$ (nm)	$\lambda_{em,\ max}$ (nm)	HOMO (eV)	E_T (eV)
CBP	78	284	453	294, 319	375	5.7	2.64
ttbCBP	175	–	478	299, 334	395	5.7	2.64

3. Results and discussion

3.1. Thermal properties and morphological stability

We used differential scanning calorimetry (DSC) and thermogravimetric analysis (TGA) to investigate the thermal properties of CBP and ttbCBP as summarized in Table 1. Fig. 1 displays the TGA thermogram and DSC curve of ttbCBP. TGA revealed that the onset decomposition temperature of ttbCBP was 404 °C, followed by 5% weight loss at 478 °C (T_d, decomposition temperature). During DSC measurements, ttbCBP underwent a glass transition at a relatively high temperature (T_g=175 °C) and showed no further phase transition upon heating up to 350 °C which means ttbCBP did not undergo recrystallization or melting. The higher value of T_d and T_g for ttbCBP, with respect to those of CBP (T_d=453 °C, T_g=78 °C) is presumably the result of its bulky and rigid molecular conformation, which is essential for morphological stability of thin films.

The thin-film morphological stability is very sensitive to pin-hole formation due to crystallization or any interfacial change that might

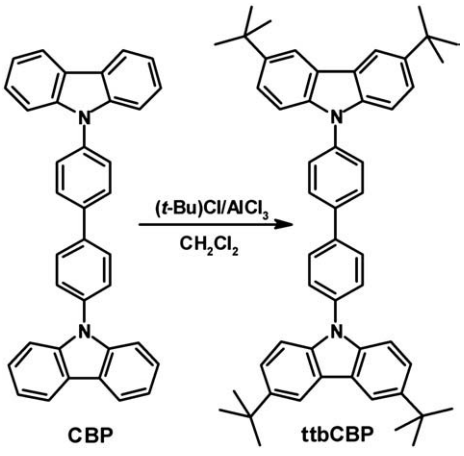

Scheme 1. Synthesis of ttbCBP.

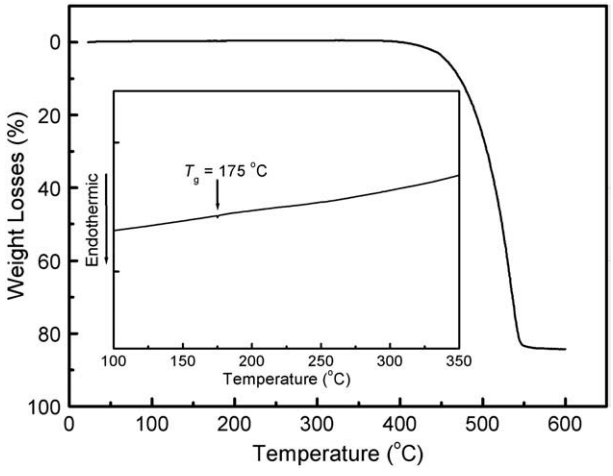

Fig. 1. TGA thermogram of ttbCBP. Inset: DSC trace of ttbCBP.

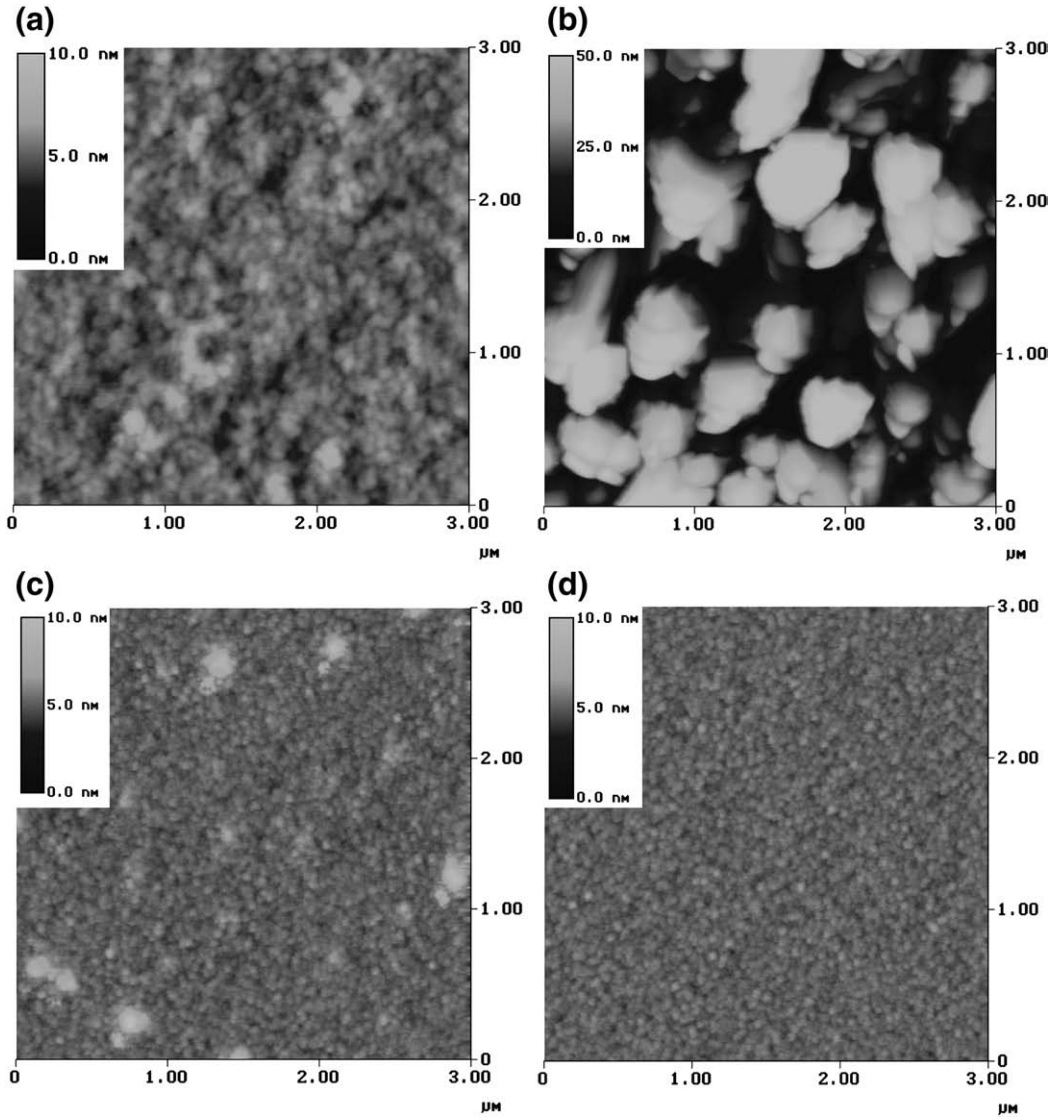

Fig. 2. AFM topographic images of CBP and ttbCBP thin films deposited on silicon wafers (50 nm). (a) CBP before heating; (b) CBP after heating; (c) ttbCBP before heating; (d) ttbCBP after heating (scanned area: 3 μm×3 μm).

be induced by Joule heating [25] during device operation which may in turn impact adversely on the lifetime of the device. The results of atomic force microscopy (AFM) measurements as shown in Fig. 2 indicated that an evaporated film of ttbCBP possessed a uniform surface that did not undergo any morphological changes when heated at 95 °C for 1 h. The root-mean-square surface roughnesses of unheated/heated ttbCBP films were 0.55 nm/0.38 nm, respectively. On the other hand, the root-mean-square surface roughnesses of unheated CBP films was 0.70 nm, and the degradation of surface morphology can be clearly observed after heated at 95 °C for 1 h. Consequently, ttbCBP forms an amorphous glass that is more stable under anticipated Joule heating. Due to the high thermal properties and morphological stability of ttbCBP, we are able to form homogenous and stable amorphous thin films of ttbCBP through vacuum evaporation.

3.2. Photo-physical properties and energy levels consideration

The photo-physical properties of CBP and ttbCBP are also summarized in Table 1. Fig. 3 compares the absorption and photoluminescence spectra of CBP and ttbCBP in $CHCl_3$. The features of the lowest absorption band and fluorescence of ttbCBP are very similar to those of CBP, except they are 15–20 nm red-shifted. Such a red red-shift is similar to what has been observed in carbazoles moiety with quaternary carbon substitutions at C-3 and C-6 positions [26,27].

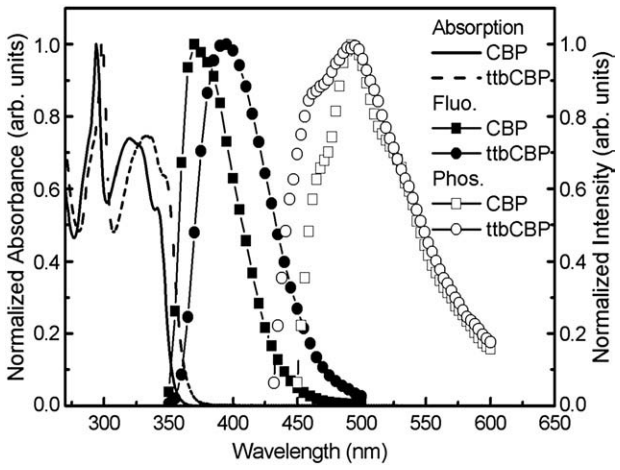

Fig. 3. Normalized absorbance, photoluminescence and phosphorescence spectra of CBP and ttbCBP.

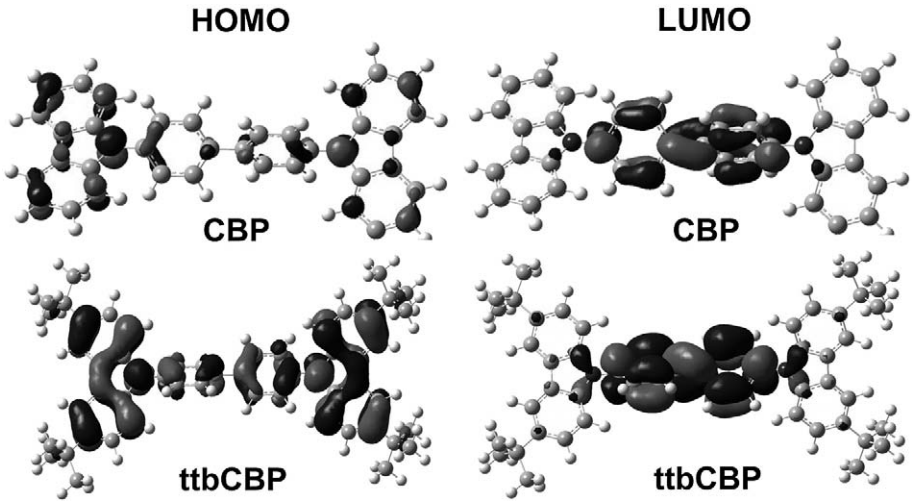

Fig. 4. The calculated HOMO/LUMO electron distribution of CBP and ttbCBP.

The calculated HOMO and LUMO electron distribution of CBP and ttbCBP as shown in Fig. 4 indicate that the filled π orbitals (or HOMO level) of CBP are located on the peripheral carbazole moieties and the unfilled π* orbitals (or LUMO level) are on the biphenyl core. It can be clearly observed that the electron distribution of ttbCBP is more delocalized with respect to that of CBP, especially the HOMO level, when introducing *t*-butyl substituents at C-3 and C-6 positions of both carbazole moieties. We believe this is primarily due to the electron-donating property of the quaternary carbon substitutions which could also be the reason for the red-shift of optical spectra. The ionization potential of CBP and ttbCBP are all 5.7 eV as determined by the UV photoelectron spectroscopy (Model AC-2). The absorption onset energy together with ionization energy provide the estimation of HOMO/LUMO energy levels of CBP and ttbCBP to be 5.7/2.4 eV and 5.7/2.5 eV, respectively.

3.3. Triplet energy

To evaluate the potential of ttbCBP as a host for electrophosphorescent devices, phosphorescence spectrum of ttbCBP was measured at 77 K in 2-methyl tetrahydrofuran glass as shown in Fig. 3. A well-characterized emission from the triplet state of ttbCBP in the region of 440–600 nm is observed, in which the first vibronic transition ($T_1^{v=0} \rightarrow S_1^{v=0}$) of the phosphorescence is assigned as the triplet energy (E_T) [28]. The E_T of ttbCBP is estimated to be ca. 2.64 eV which is identical to that of CBP [29], suggesting that ttbCBP can be used as host material for triplet green and red emitters. These photophysical results clearly indicate that despite the introduction of *t*-butyl substituents which result in a slightly narrower band-gap, the sterically hindered spacers give ttbCBP molecule with surprisingly robust morphological stability and most importantly it preserves the high triplet energy.

3.4. Device performance

The detailed electroluminescent (EL) performances measured at 20 mA/cm^2 are summarized in Table 2, the EL efficiency of ttbCBP-host devices are comparable to those of CBP-host devices B and D. Devices A and C obtained a maximum E. Q. E. of 8.3% with 28.8 cd/A and 16.4 lm/W at 0.5 mA/cm^2 and 9.8% with 6.7 cd/A and 3.0 lm/W at 2 mA/cm^2, respectively, The high EL efficiency can be attributed to the E_T of ttbCBP (~2.64 eV) which is higher than that of Ir(ppy)$_3$ (~2.42 eV) and Ir(piq)$_3$ (~2.0 eV), ensuring that the triplet energy transfer from ttbCBP to Ir(ppy)$_3$ or Ir(piq)$_3$ is *exothermic* and that the transferred excitons are well confined on the iridium dopants. As a result, devices A and C exhibit pure EL peaks at 512 nm from Ir(ppy)$_3$ and 628 nm from Ir(piq)$_3$, respectively. Furthermore, no emission from ttbCBP is observed, indicative of complete energy transfer from ttbCBP to the green and red iridium phosphors in the emitting layer.

Table 2
EL performances of four electrophosphorescent devices driven at 20 mA/cm^2

Device (host)	Voltage (V)	Luminance (cd/m^2)	Current Eff. (cd/A)	E. Q. E. (%)	Peak (nm)	CIE (x, y)
A (ttbCBP)	9.6	4983	24.9	7.3	512	(0.31, 0.62)
B (CBP)	8.4	4935	24.6	7.2	512	(0.30, 0.62)
C (ttbCBP)	11.7	1181	5.9	8.6	628	(0.68, 0.32)
D (CBP)	10.0	1282	6.4	9.2	628	(0.68, 0.32)

Fig. 5 shows the E. Q. E. versus voltage characteristics of these electrophosphorescent devices. All devices show a gradual decrease in EL efficiency with voltage, which is often observed in phosphorescent OLEDs and is usually attributed to triplet–triplet annihilation [30]. Nevertheless, as the drive voltage was increased to 16 V, E. Q. E. of ttbCBP-host devices A and C remains above 5%, which are still substantially higher than that of fluorescent green and red OLED device (3–5%). Furthermore, ttbCBP-host devices appear to less efficiency roll-off than that obtained with the CBP-host devices, which is presumably due to the high morphological stability of ttbCBP thin film and thus alleviate EL efficiency quenching under high voltage.

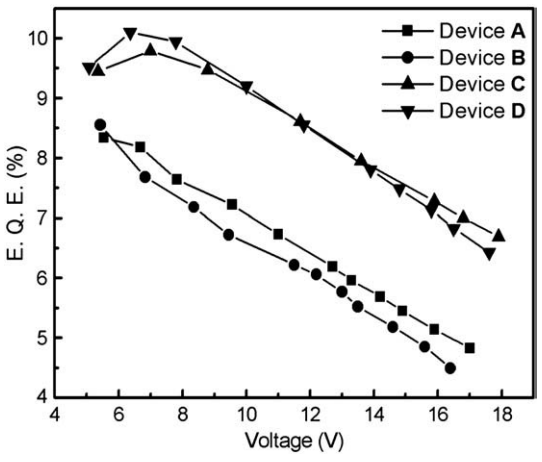

Fig. 5. E. Q. E. versus voltage characteristics of devices A, B, C and D.

4. Conclusion

We have discovered a host material for green and red triplet emitters — 4,4′-*N*,*N*′-[di(3,6-di(*t*-butyl)carbazole]biphenyl (ttbCBP) synthesized through a facile route, which is based on the design strategy of steric substitution on peripheral carbazole moieties of CBP. The introduction of the *t*-butyl substituents significantly improve the thermal and morphological stability of amorphous thin film and preserve the high triplet energy of the molecule. Green $Ir(ppy)_3$ and red $Ir(piq)_3$ doped phosphorescent OLEDs with ttbCBP as host material show remarkable external quantum efficiencies and less efficiency roll-off at high drive voltage.

Acknowledgements

This work was supported by grants from Chunghwa Picture Tubes, Ltd. (CPT) and National Science Council of Taiwan. We also thank e-Ray Optoelectronics Technology Co., Ltd. of Taiwan for supplying some of the OLED materials studied in this work.

References

[1] M.A. Baldo, D.F. O'Brien, A. Shoustikov, S. Sibley, M.E. Thompson, S.R. Forrest, Nature 395 (1998) 151.
[2] M.A. Baldo, M.E. Thompson, S.R. Forrest, Nature 403 (2000) 750.
[3] S. Lamansky, P.I. Djurovich, D. Murphy, F. Abdel-Razzaq, R. Kwong, I. Tsyba, M. Bortz, B. Mui, R. Bau, M.E. Thompson, Inorg. Chem. 40 (2001) 1704.
[4] S. Lamansky, P. Djurovich, D. Murphy, F. Abdel-Razzaq, H.E. Lee, C. Adachi, P.E. Burrows, S.R. Forrest, M.E. Thompson, J. Am. Chem. Soc. 123 (2001) 4303.
[5] C.F. Chen, G. He, Y. Yang, Appl. Phys. Lett. 82 (2003) 1006.
[6] M. Sudhakar, P.T. Djurovich, T.E. Hogen-Esch, M.E. Thompson, J. Am. Chem. Soc. 123 (2003) 7796.
[7] D.F. O'Brien, M.A. Baldo, M.E. Thompson, S.R. Forrest, Appl. Phys. Lett. 74 (1999) 442.
[8] C. Adachi, M.A. Baldo, S.R. Forrest, S. Lamansky, M.E. Thompson, R.C. Kwong, Appl. Phys. Lett. 78 (2001) 1622.
[9] M.A. Baldo, S. Lamansky, P.E. Burrows, M.E. Thompson, S.R. Forrest, Appl. Phys. Lett. 75 (1999) 4.
[10] C. Adachi, R.C. Kwong, S.R. Forrest, Org. Electron. 2 (2001) 37.
[11] A. Tsuboyama, H. Iwawaki, M. Furugori, T. Mukaide, J. Kamatani, S. Igawa, T. Moriyama, S. Miura, T. Takiguchi, S. Okada, M. Hoshino, K. Ueno, J. Am. Chem. Soc. 125 (2003) 12971.
[12] S. Tokido, H. Tanaka, N. Noda, A. Okada, T. Taga, Appl. Phys. Lett. 70 (1997) 1929.
[13] P. Fenter, F. Schreiber, V. Buloviæ, S.R. Forrest, Chem. Phys. Lett. 277 (1997) 521.
[14] B.W. D'Andrade, S.R. Forrest, A.B. Chwang, Appl. Phys. Lett. 83 (2003) 3858.
[15] S.J. Yeh, W.C. Wu, C.T. Chen, Y.H. Song, Y. Chi, M.H. Ho, S.F. Hsu, C.H. Chen, Adv. Mater. 17 (2005) 285.
[16] P.I. Shih, C.L. Chiang, A.K. Dixit, C.K. Chen, M.C. Yuan, R.Y. Lee, C.T. Chen, E.W.G. Diau, C.F. Shu, Org. Lett. 8 (2006) 2799.
[17] M.H. Tsai, H.W. Lin, H.C. Su, T.H. Ke, C.C. Wu, F.C. Fang, Y.L. Liao, K.T. Wong, C.I. Wu, Adv. Mater. 18 (2006) 1216.
[18] K.T. Wong, Y.M. Chen, Y.T. Lin, H.C. Su, C.C. Wu, Org. Lett. 7 (2005) 5361.
[19] Y.C. Chen, G.S. Huang, C.C. Hsiao, S.A. Chen, J. Am. Chem. Soc. 128 (2006) 8549.
[20] C. Friedel, J.M. Crafts, Compt. Rend. 84 (1877) 1392.
[21] C. Lee, W. Yang, R.G. Parr, Phys. Rev., B 37 (1988) 785.
[22] M.J. Frisch, G.W. Trucks, H.B. Schlegel, G.E. Scuseria, M.A. Robb, J.R. Cheeseman, J.A. Montgomery Jr., T. Vreven, K.N. Kudin, J.C. Burant, J.M. Millam, S.S. Iyengar, J. Tomasi, V. Barone, B. Mennucci, M. Cossi, G. Scalmani, N. Rega, G.A. Petersson, H. Nakatsuji, M. Hada, M. Ehara, K. Toyota, R. Fukuda, J. Hasegawa, M. Ishida, T. Nakajima, Y. Honda, O. Kitao, H. Nakai, M. Klene, X. Li, J.E. Knox, H.P. Hratchian, J.B. Cross, C. Adamo, J. Jaramillo, R. Gomperts, R.E. Stratmann, O. Yazyev, A.J. Austin, R. Cammi, C. Pomelli, J.W. Ochterski, P.Y. Ayala, K. Morokuma, G.A. Voth, P. Salvador, J.J. Dannenberg, V.G. Zakrzewski, S. Dapprich, A.D. Daniels, M.C. Strain, O. Farkas, D.K. Malick, A.D. Rabuck, K. Raghavachari, J.B. Foresman, J.V. Ortiz, Q. Cui, A.G. Baboul, S. Clifford, J. Cioslowski, B.B. Stefanov, G. Liu, A. Liashenko, P. Piskorz, I. Komaromi, R.L. Martin, D.J. Fox, T. Keith, M.A. Al-Laham, C.Y. Peng, A. Nanayakkara, M. Challacombe, P.M.W. Gill, B. Johnson, W. Chen, M.W. Wong, C. Gonzalez, J.A. Pople, Gaussian 03, Revision A.1, Gaussian, Inc., Pittsburgh PA, 2003.
[23] L.S. Hung, L.R. Zheng, M.G. Mason, Appl. Phys. Lett. 78 (2001) 673.
[24] S.A. Van Slyke, C.H. Chen, C.W. Tang, Appl. Phys. Lett. 69 (1996) 2160.
[25] J.W. Choi, J.S. Kim, S.Y. Oh, H.W. Rhee, W.H. Lee, S.B. Lee, Thin Solid Films 363 (2000) 271.
[26] Z. Zhu, J.S. Moore, J. Org. Chem. 65 (2000) 116.
[27] N.D. McClenaghan, R. Passalacqua, F. Loiseau, S. Campagna, B. Verheyde, A. Hameurlaine, W. Dehaen, J. Am. Chem. Soc. 125 (2003) 5356.
[28] A.V. Dijken, J.J.A.M. Bastiaansen, N.M.M. Kiggen, B.M.W. Langeveld, C. Rothe, A.P. Monkman, I. Bach, P. Stössel, K. Brunner, J. Am. Chem. Soc. 126 (2004) 7718.
[29] R.J. Holmes, S.R. Forrest, Y.J. Tung, R.C. Kwong, J.J. Brown, S. Garon, M.E. Thompson, Appl. Phys. Lett. 82 (2003) 2422.
[30] M.A. Baldo, C. Adachi, S.R. Forrest, Phys. Rev., B 62 (2000) 10967.